JOC The Journal of Organic Chemistry

Article

pubs.acs.org/joc

Mechanisms for the Formation of Acenes from α-Diketones by Bisdecarbonylation

Holger F. Bettinger,*[,†] Rajib Mondal,[‡] Małgorzata Krasowska,[†] and Douglas C. Neckers[‡]

[†]Institut für Organische Chemie, Universität Tübingen, Auf der Morgenstelle 18, 72076 Tübingen, Germany

[‡]Center for Photochemical Sciences, Bowling Green State University, Bowling Green, Ohio 43403, United States

Supporting Information

ABSTRACT: The bisdecarbonylation of bridged α-diketones has turned into an important reaction for the photochemical generation of higher acenes, in particular under matrix isolation conditions. Here, a computational mechanistic analysis of the bisdecarbonylation of dibenzobicyclo[2.2.2]-octadienedione **2** to anthracene **1** is presented. The study employed the B3LYP functional in conjunction with the 6-311+G** basis set for geometry optimization on the S_0, S_1, and T_1 potential energy surfaces as well as coupled cluster [CCSD(T)] and second-order multireference perturbation theory (MRMP2) with the cc-pVDZ basis set for evaluation of energies of intermediates and transition states. The first step of the most favorable pathway on the T_1 surface has a barrier of 12 kcal mol^{-1} with respect to the T_1 minimum **2**-$^3B_1$ and involves cleavage of the C−C bond between the bridgehead and one carbonyl atom, C_{bridge}−C(O), yielding a biradical intermediate (**INT1-T**). On the S_1 surface, the analogous step only has a barrier of less than 4 kcal mol^{-1}. A conical intersection of the S_1 with the S_0 surface exists after the transition state and provides a means for relaxation to a biradical intermediate (**INT1-S**) on the S_0 surface. The concerted loss of two CO molecules from **INT1-S** has only a very small barrier. Similarly, consecutive loss of two CO molecules from the triplet state of this diradical (**INT1-T**) to give triplet anthracene is more favorable than ejection of triplet ethylenedione. Thus, the features identified computationally on the S_0, S_1, and T_1 potential energy surface agree with earlier experimental observations of a fast photobisdecarbonylation within 7 ns from the triplet and singlet states of **2** and a lack of triplet ethylenedione formation.

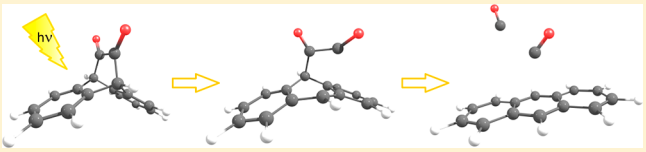

INTRODUCTION

Poly(acene)s (**1**), linear poly(benzenoid) hydrocarbons, are an important class of compounds because of their potential applications in electronic devices (Chart 1).[1−6] However, the synthesis of the higher molecular weight polyacenes has proven particularly problematic due to their inherent instability, and this has limited their study. For example, kinetically stabilized heptacenes (**1**, n = 7)[7−10] and nonacenes (**1**, n = 9),[11,12] the largest known member of the poly(acene)s, have only recently been reported.

Chart 1

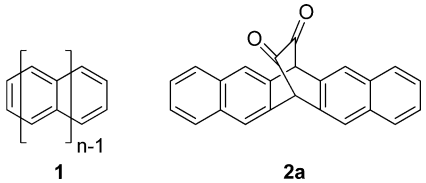

1 **2a**

In the search for soluble pentacene precursors, Ono et al.[13,14] described in 2005 that 6,13-dihydro-6,13-ethanopentacene-15,16-dione (**2a**, see Chart 1) decarbonylates to pentacene (**1**: n = 5) in high yield upon visible light irradiation in toluene solution (Scheme 1). The α-diketone protecting group has since been used in a number of studies.[15−22] It also proved important in the photochemical synthesis of hexacene (**1**: n = 6),[23] which was recently generated also thermally,[24] and heptacene (**1**: n = 7).[25] The photodecomposition of α-diketones also allowed the study of the spectral properties of the higher acenes up to nonacene along with their radical ions in inert gas matrices.[26−28]

Scheme 1. Photobisdecarbonylation of 9,10-Dihydro-9,10-ethanoanthracene-11,12-dione (2) Yields Anthracene 1 (n = 3)[29]

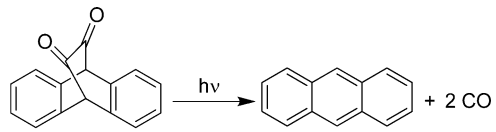

2 **1**

The photodecarbonylation of α-diketones **2** was first reported in 1969 by Strating et al.,[29] and it is sometimes called the Strating−Zwanenburg reaction. These authors observed the quantitative formation of anthracene from 9,10-dihydro-9,10-ethanoanthracene-11,12-dione (**2**) and recognized its unusual

Special Issue: Howard Zimmerman Memorial Issue

Received: August 1, 2012
Published: October 11, 2012

   dx.doi.org/10.1021/jo301622f | J. Org. Chem. 2013, 78, 1851−1857

course. In case of aliphatic diketones, e.g., biacetyl, camphor quinone, and benzil, photoreduction via electron transfer is generally followed by proton transfer to the radical anion.[30−33] Further investigations by Rubin and his group substantiated the unusual nature of this photoreaction.[34−36]

The detailed mechanism of the photobisdecarbonylation of α-diketones **2**, however, is yet to be delineated. The photoprecursors **2** actually undergo expulsion of two molecules of carbon monoxide upon irradiation, and Strating et al.[29] speculated based on the mass spectra that the photochemical expulsion of the diketo bridge occurs through extrusion of ethylenedione, C_2O_2. This elusive molecule could, however, not be detected during the decomposition of related bridged α-diketones in a matrix isolation study.[37] A comprehensive study by Schröder et al.[38] revealed that ethylenedione, a ground-state triplet molecule,[39] is intrinsically short-lived with a lifetime at most in the lower nanosecond range.

Recently, time-resolved nanosecond laser flash photolysis (LFP) and femtosecond pump−probe UV−vis spectrometric techniques along with steady-state photolysis have been carried out to understand the mechanism of the Strating−Zwanenburg photodecarbonylation of α-diketone precursors of anthracene, hexacene, and heptacene.[40] It was found that both the singlet and the triplet states of the diketones are involved in the decarbonylation process that occurs within the subnanosecond time scale.[40] The photobisdecarbonylation is indeed so fast that it is complete within the width of the laser pulse (7 ns), and thus, no intermediate could be detected. In agreement with Schröder et al.,[38] no evidence for the formation of ethylenedione was found.

The question as to whether the bisdecarbonylation proceeds in a concerted or stepwise fashion is an intriguing one. The experimental investigations could not shed light on the initial step of the reaction so far, and it is therefore not clear if the bond between the carbonyl atoms, (O)C−C(O), or that between a bridgehead and a carbonyl atom, C_{bridge}−C(O), breaks first. The fast reaction implies low barriers on the potential energy surfaces, but barrier heights are not available from experiment and theory at this time. Inspired by the limited availability of data and the importance of the Strating−Zwanenburg reaction for the synthesis of acenes in our research groups, we have undertaken a theoretical investigation of this reaction on the S_0, S_1, and T_1 potential energy surfaces.

COMPUTATIONAL DETAILS

The geometries of stationary points on the ground state singlet (S_0) and triplet (T_1) potential energy surfaces (PES) were completely optimized within the given point group constraints at the B3LYP[41,42] level of theory as implemented[43] in the Gaussian 09[44] program system in conjunction with the 6-31G*[45,46] and 6-311+G**[47] basis sets. Geometries on the S_1 PES were optimized using time-dependent[48−50] theory with the same functional and basis sets. Computation of harmonic vibrational frequencies, analytically for the S_0 and T_1 PES, but by finite differences of analytic gradients for the S_1 PES, with the 6-31G* basis set confirmed that the obtained structures correspond to minima and transition states. The spin-unrestricted treatment (abbreviated as UB3LYP) was used for the triplet manifold. Structures on the S_0 surface were treated with UB3LYP if a triplet instability could be detected.[51] All geometries discussed in the text were obtained at the (U)B3LYP/6-311+G** level of theory, while zero-point vibrational energy corrections and Gibbs free enthalpies at 298.15 K were computed at the B3LYP/6-31G* level.

Energies were refined by single point computations using the B3LYP/6-311+G** geometries. Unless noted otherwise, these refinements were performed using coupled cluster theory considering single, double, and a perturbative estimate of triple excitations, CCSD(T).[52] Spin-unrestricted Hartree−Fock references and a spin-unrestricted CC treatment (UHF-UCCSD(T)) were used for the high-spin stationary points. The frozen-core approximation was employed. Dunning's[53] correlation consistent cc-pVDZ basis set was used for CCSD(T) computations.

As most of the stationary points on the S_0 potential energy surface proved to have pronounced multireference character, the performance of CCSD(T) theory may be doubtful. Hence, second-order multireference perturbation theory (MRMP2)[54−60] was used for refining the energies at the UB3LYP/6-311+G** geometries. The broken-symmetry UHF solution gave 16 orbitals with occupation numbers between 1.98 and 0.02 for the three stationary points located. Following the suggestion of Pulay and Hamilton,[61] a 16 × 16 CASSCF treatment would be indicated, and that is clearly too large to be computationally feasible. We thus decided to include only the two most important electrons and orbitals resulting in a CASSCF(2,2) wave function as a basis for the second-order perturbation treatment. To be able to compare the energies of the T_1 PES (that were obtained at the CCSD(T) level) and S_0 (MRMP2), the decisive intermediate on the triplet PES, **INT1-T**, was also computed at the CAS(2,2)-MRMP2 level of theory. For the triplet state, the CASSCF(2,2) treatment corresponds to a single configuration and MRMP2 is identical to MP2. The CASSCF and MRMP2 computations were performed with GAMESS-US.[62]

To summarize, unless noted otherwise, energies mentioned in the text were obtained at the (U)CCSD(T)/cc-pVDZ//(U)B3LYP/6-311+G** + ZPVE(B3LYP/6-31G*) level of theory.

RESULTS AND DISCUSSION

Electronic Structure of the α-Diketone 2. Geometry optimization of **2** in its electronic ground state ($^1A_1$) results in a minimum of C_{2v} symmetry. The highest occupied molecular orbital (HOMO) is bonding between the bridgehead and carbonyl carbon atoms (Figure 1). The lowest unoccupied molecular orbital (LUMO), on the other hand, is a π-type orbital of the C_2O_2 unit and is bonding between the carbonyl atoms. Excitation from the HOMO of a_1 symmetry to the LUMO of b_1 symmetry gives rise to the $^1B_1$ and $^3B_1$ states. These are the lowest energy excited states of **2**. The triplet is 53.5 kcal mol^{-1} higher in energy than the ground state according to the experimental investigation of Mondal et al.[40] We compute an adiabatic energy difference of $\Delta_{298.15}G$ = 54.1 kcal mol^{-1} [CCSD(T)], while the vertical energy difference is somewhat larger (61 kcal mol^{-1}). The lowest energy $^3A_2$, $^3B_2$,

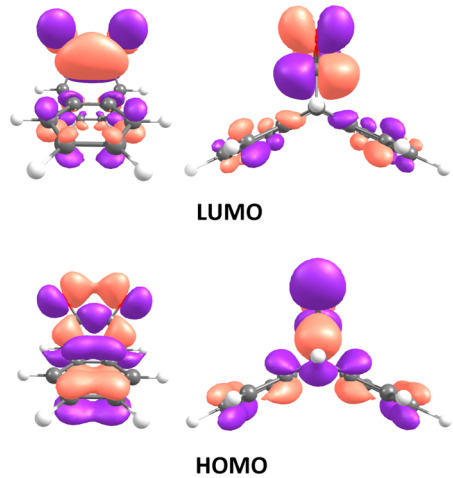

Figure 1. HOMO and LUMO of **2**-$^1A_1$ as computed at the B3LYP/6-31G* level of theory.

dx.doi.org/10.1021/jo301622f | J. Org. Chem. 2013, 78, 1851−1857

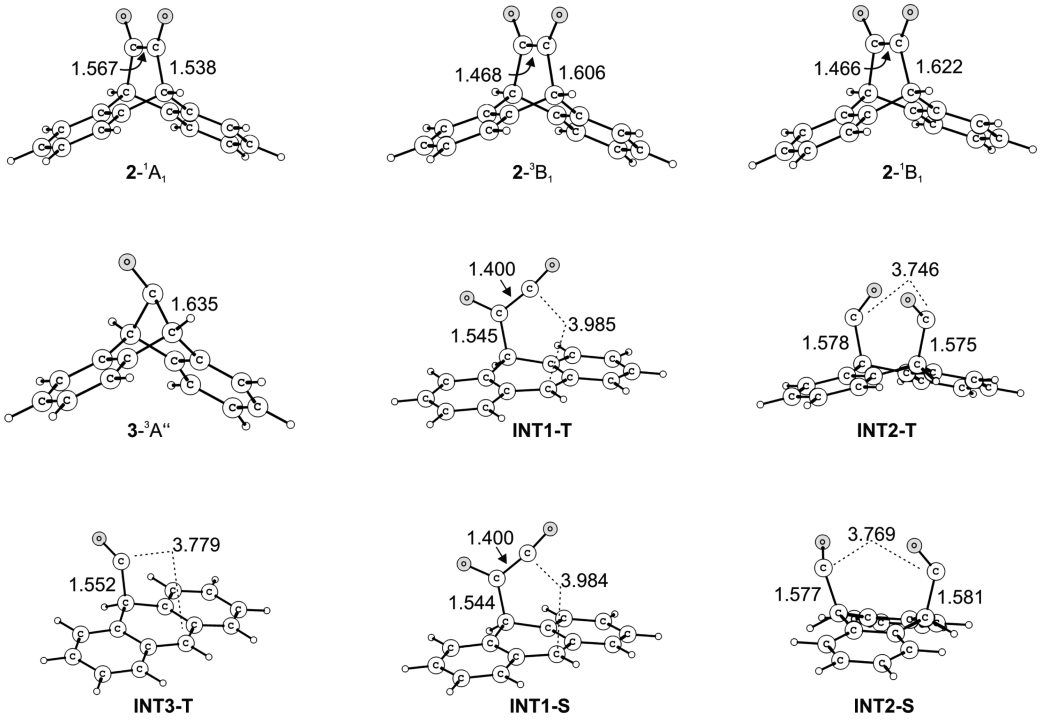

Figure 2. Geometries of minima optimized at the (U)B3LYP/6-311+G** level of theory. Distances between bridgehead and carbonyl carbon atoms are given in Å.

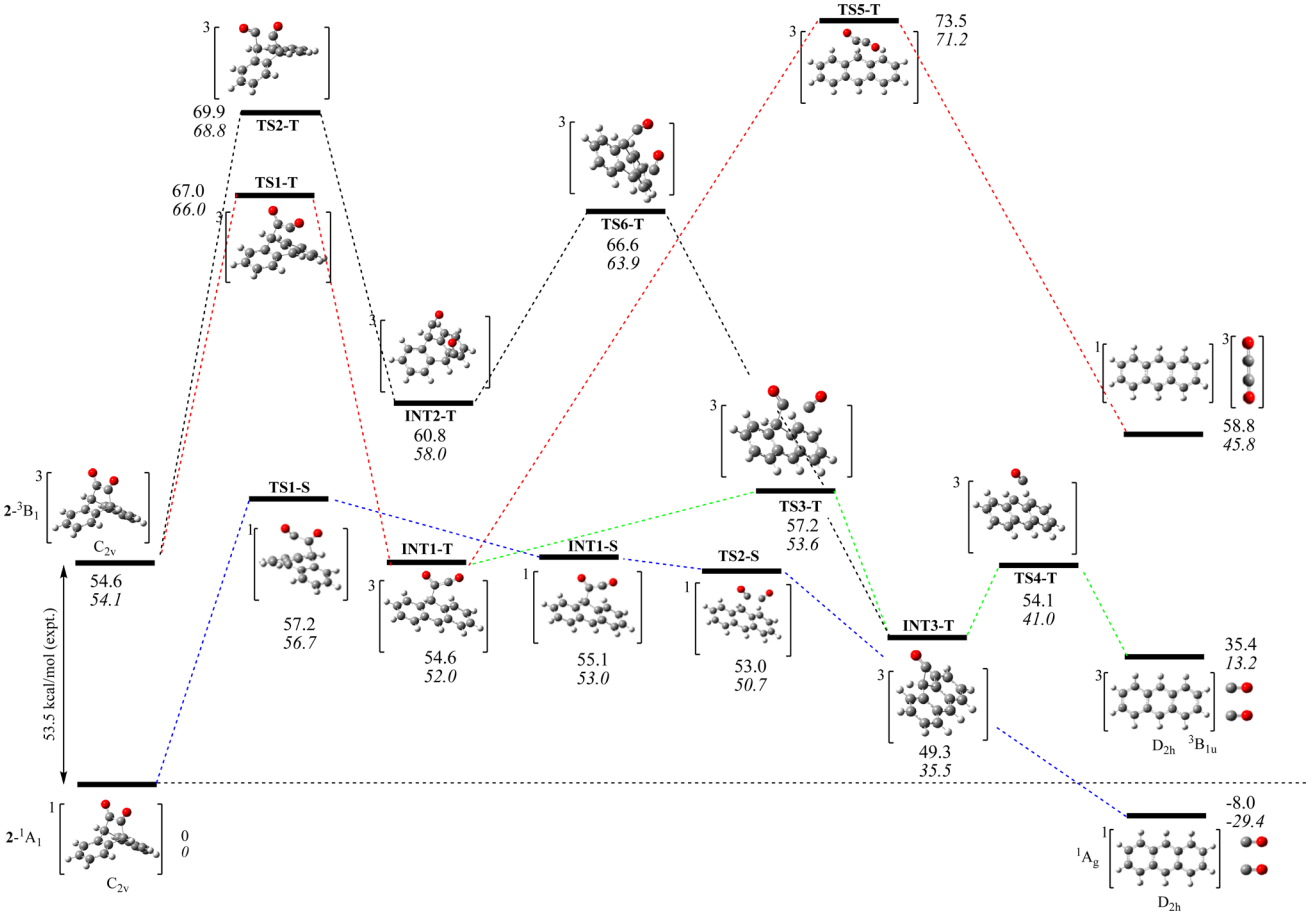

Figure 3. Relative energies (ZPVE corrected, in kcal mol^{-1}) and $\Delta_{298.15}G$ (in kcal mol^{-1}, italics) computed for bisdecarbonylation of **2** (not drawn to scale) at CCSD(T)/cc-pVDZ and CAS(2,2)-MRMP2/cc-pVDZ (**TS1-S**, **INT1-S**, **TS2-S**) levels at B3LYP/6-311+G** geometries.

dx.doi.org/10.1021/jo301622f | J. Org. Chem. 2013, 78, 1851−1857

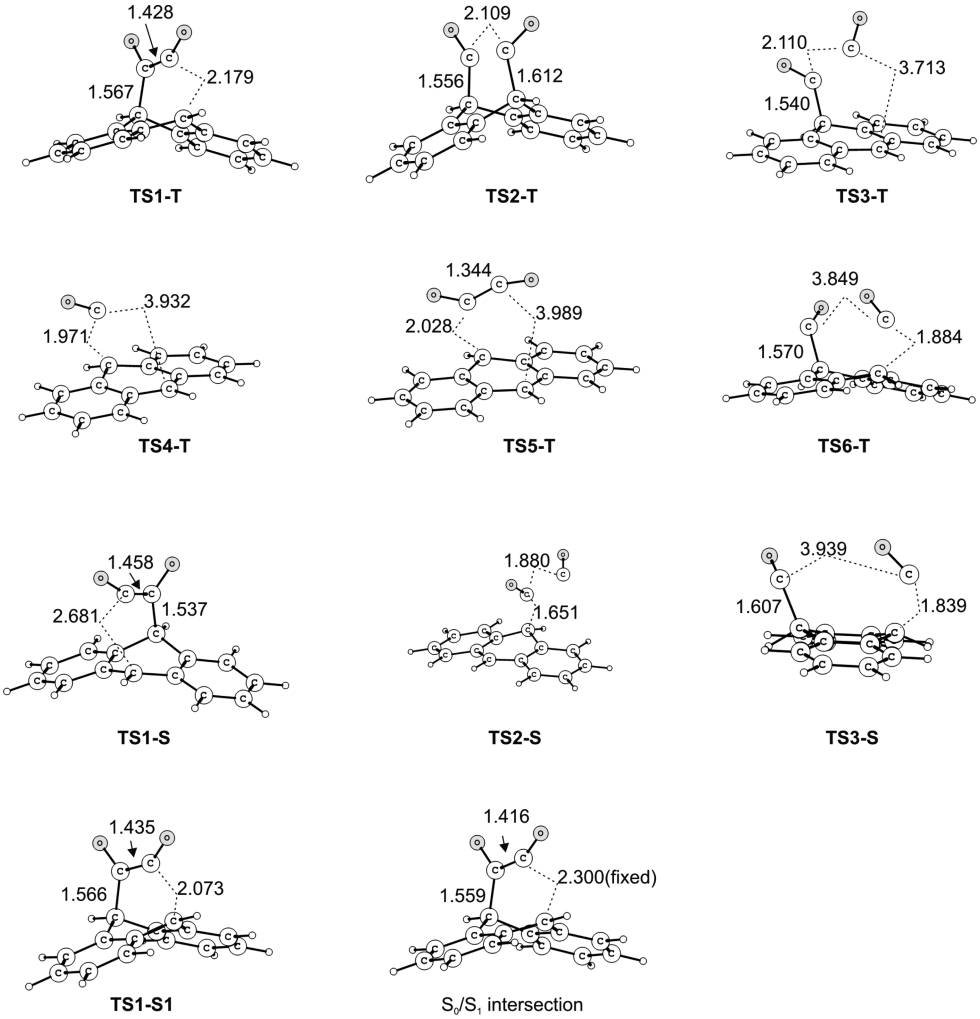

Figure 4. Geometries of transition structures optimized at the (U)B3LYP/6-311+G** and TD-B3LYP/6-311+G** (**TS1-S1**; approximate S_0/S_1 intersection) levels of theory. Distances between bridgehead and carbonyl carbon atoms are given in Å.

and $^3A_1$ states are much higher in energy (83−102 kcal mol^{-1}, B3LYP/6-311+G** data) and need not be considered further.

The transition from the ground state to the $^1B_1$ state is optically allowed, and this corresponds to the longest wavelength absorption of **2**. The experimental energy of this S_1 state is 58.0 kcal mol^{-1}.[40] The computed (B3LYP/6-311+G**) vertical energy difference is 58.1 kcal mol^{-1}, and this decreases to 52.4 kcal mol^{-1} after optimization of the S_1 state geometry. Hence the calculations are in good agreement with experiment and confirm that the S_1 and T_1 states of **2** differ only by a few kcal mol^{-1}.

As in both the $^1B_1$ and $^3B_1$ states an electron is excited out of an orbital that is bonding with respect to the bridgehead−carbonyl bond and into an orbital that is bonding between the carbonyl atoms, the corresponding bonds lengthen and shorten, respectively. The lengthening of the C_{bridge}−C(O) bond amounts to 1.606 Å ($^3B_1$) and 1.622 ($^1B_1$) from 1.538 Å in **2**-$^1A_1$ (see Figure 2 for geometries). The (O)C−C(O) bond shortens to 1.468 Å ($^3B_1$) and 1.466 ($^1B_1$) from 1.567 Å in **2**-$^1A_1$. Hence, it may be expected that the cleavage of the stretched C_{bridge}−C(O) is easier than that of the (O)C−C(O) bond in these excited states.

Energy Balance. The bisdecarbonylation of singlet **2** to give anthracene and two molecules of CO, each in their electronic ground state, is computed to be mildly exothermic, ΔE = −8.0 kcal mol^{-1}. The formation of anthracene in its lowest energy triplet electronic state is endothermic by 35.4 kcal mol^{-1}; the computed S-T energy splitting of anthracene at our level of theory, 42.4 kcal mol^{-1}, in good agreement with the experimental (42.5 kcal mol^{-1}) one.[63]

Alternatively, the formation of anthracene and ethylenedione can be considered. The latter is a ground state triplet molecule. The lowest energy form in the singlet manifold is a linear open-shell singlet state, $^1\Delta_g$ in D_{2h} symmetry. The previous computations by Korkin et al. have shown that this state, however, is unstable towards dissociation into two molecules of CO.[64] Consequently, dissociation of **2** into **1** and singlet C_2O_2 is excluded even theoretically. The repulsive C_2O_2 singlet potential energy surfaces crosses the triplet state surface close to the triplet ground state minimum, and hence Schröder et al.[38] concluded that ethylenedione should only have a lifetime in the nanosecond range. The formation of anthracene in its S_0 state and triplet C_2O_2 is computed to be endothermic by 63.1 kcal mol^{-1}. The energy difference between triplet C_2O_2 and two CO molecules computed at our level, 66.8 kcal mol^{-1}, compares well with the data obtained by Schröder et al.[38]

T_1 Potential Energy Surface. The energies mentioned in this section were obtained at the (U)CCSD(T)//(U)B3LYP/6-311+G** level of theory. We could locate two transition states that connect **2**-$^3B_1$ to two intermediates (see Figure 3 for

dx.doi.org/10.1021/jo301622f | J. Org. Chem. 2013, 78, 1851−1857

a schematic depiction of the PES). In the first one (**TS1-T**) the C−C bond between a bridgehead carbon atom and the adjacent carbonyl carbon breaks. It is stretched to 2.179 Å compared to 1.606 Å in the T_0 state (see Figure 4 for all TS structures discussed in this paper).

The second one (**TS2-T**) describes the breaking of the bond between the two carbonyl carbon atoms that are separated by 2.109 Å in **TS2-T**. This C(O)−C(O) bond is shorter in the triplet (1.468 Å) than it is in the S_0 state (1.567 Å). The energy of **TS2-T** is higher than that of **TS1-T** by 2.9 kcal mol^{-1}. In the two intermediates **INT1-T** and **INT2-T** that are reached from **TS1-T** and **TS2-T**, respectively, the corresponding C−C bonds are completely broken (3.985 and 3.746 Å, respectively). The energy of **INT1-T** is almost identical with that of **2**-$^3B_1$ and 6.2 kcal mol^{-1} lower than that of **INT2-T**.

From **INT1-T** two further reactions paths could be identified. The one with less energy demand (2.6 kcal mol^{-1} with respect to **INT1-T**) involves cleavage of the bond between the carbonyl groups and expulsion of singlet CO via **TS3-T**. The breaking bond is stretched to 2.110 Å in **TS3-T**. This process results in **INT3-T** + CO that lies 5.3 kcal mol^{-1} below **INT1-T**. Expulsion of the last CO molecule and formation of triplet anthracene proceeds via **TS4-T**. The distance between the departing CO and the former bridgehead atom is 1.971 Å. This last step involves a barrier of 4.8 kcal mol^{-1} and formation of triplet anthracene and two singlet CO molecules; it is exothermic by almost 14 kcal mol^{-1}.

Another conceivable path (not shown in Figure 3) starting at **INT3-T** is collapse to the bridged monoketone **3** in its triplet state. Due to the high energy of this triplet species, 85 kcal mol^{-1}, this reaction seems to be unlikely.

The second path emanating from **INT1-T** is the breaking of the bond involving the second bridgehead atom and the C_2O_2 unit via **TS5-T**. Thus this path connects to anthracene (S_0) and triplet C_2O_2. It involves a barrier of 18.9 kcal mol^{-1} and is endothermic by 4.2 kcal mol^{-1} with respect to **INT1-T**. As discussed above, triplet C_2O_2 is not expected to be stable, and energy can be gained by its fragmentation into two CO molecules.

From **INT2-T**, expulsion of one of the two CO groups proceeds via **TS6-T**. In **TS6-T**, the distance between the CO carbon atom and the bridgehead atom is stretched to 1.884 Å. The reaction involves a barrier of 5.8 kcal mol^{-1} and leads downhill to **INT3-T** that is 11.5 kcal mol^{-1} more stable than **INT2-T**. Decomposition of **INT3-T** can then proceed as discussed above.

S_0 Potential Energy Surface. Explorative computations revealed significant multireference character, hence final energies were obtained at the CASSCF(2,2)-MRMP2/cc-pVDZ//(U)B3LYP/6-311+G** level of theory. We first focus on the lowest energy intermediate **INT1** that we identified on the triplet PES. Computations of **INT1-S** starting at the geometry of **INT1-T** revealed a triplet instability of the spin-restricted (RB3LYP) description, and thus, the spin-unrestricted approach (UB3LYP) was used ($<S^2>$ = 1.04, 0.30 after annihilation). Geometry optimization resulted in an intermediate **INT1-S** that has a structure and energy similar to **INT1-T** to within 0.3 kcal mol^{-1} at the B3LYP/6-311+G** level of theory. As both UB3LYP and CCSD(T) energies of **INT1-S** may be unreliable, multireference (MR) MP2 computations were employed as described in the Computational Details. At this level of theory, the singlet is less stable than the triplet by 0.5 kcal mol^{-1}, in good agreement with the UB3LYP result.

A transition structure **TS1-S** could be located that connects **INT1-S** to the α-diketone. Again, a spin-unrestricted treatment ($<S^2>$ = 0.78, 0.14 after annihilation) produces a lower energy structure than the spin-restricted solution. The structure of **TS1-S** thus obtained is similar to the analogous structure on the triplet manifold (**TS1-T**) with a distance between the carbon atoms of the breaking bond of 2.681 Å. The energy of **TS1-S** at the CAS(2,2)-MRMP2 level is 2.6 kcal mol^{-1} higher than that of **INT1-T**. Using the energy of **INT1-T** at the CCSD(T) level as reference point (54.6 kcal mol^{-1}), a barrier of 57.2 kcal mol^{-1} with respect to the α-diketone **2**-S_0 is obtained.

The decarbonylation from **INT1-S** can proceed through **TS2-S** that could be located at the UB3LYP/6-311+G** level of theory ($<S^2>$ = 0.60, 0.09 after annihilation). In **TS2-S** the distance between the carbonyl carbon atoms is stretched (1.880 Å), while at the same time the distance between the bridgehead and carbonyl carbons is elongated to 1.651 Å. The transition vector corresponds to breaking of both the OC−CO as well as the OC−C_{bridge} bonds. Hence, **TS2-S** is associated with loss of two molecules of CO from **INT1-S**. At the B3LYP/6-311+G** level **TS2-S** is 4.3 kcal mol^{-1} higher in energy than **INT1-S**, but using MRMP2, the energy of **TS2-S** drops below that of **INT1-S**. This indicates that **INT1-S** is most likely a rather unstable intermediate that quickly loses its two CO carbonyl groups.

An intermediate that is analogous to **INT2-T** also exists on the S_0 potential energy surface (**INT2**-S). The (O)C−C(O) bond is broken (3.769 Å) in **INT2-S**. This intermediate (not shown in Figure 3 for clarity) lies higher in energy than **INT1-S** by 13.3 kcal mol^{-1}. All our attempts to locate the transition structure that connects **INT2-S** to **2**-$^1A_1$ unfortunately failed at the UB3LYP level of theory, presumably due to the challenging electronic structure of such a bond breaking TS. But as **TS1-S** is at least 11 kcal mol^{-1} lower in energy than any transition state leading to **INT2-S**, a pathway involving **INT2-S** is unlikely to be competitive experimentally. For completeness sake, we investigated loss of carbonyl groups from **INT2-S** and found a transition state **TS3-S** that is only 0.1 kcal mol^{-1} above **INT2-S** in energy. This connects **INT2-S** to anthracene and two CO molecules.

S_1 Potential Energy Surface. Photoirradiation will excite the molecule electronically and after fast relaxation, possibly electronic and vibrational, the S_1 surface will be reached (**2**-$^1B_1$). Here, in particular, the first transition state of decomposition of **2**-$^1B_1$ and the existence of a conical intersection that allows fast transition to the S_0 surface are of importance. We describe this part of the S_1 PES using TD-DFT (B3LYP/6-311+G**) and CASSCF(2,2).

The asynchronous breaking of the C_{bridge}−C(O) bond reduces the symmetry from C_{2v} to C_s. Within the constraint of the molecular framework to the C_s point group, the symmetry species of the ground state is A′ and that of the S_1 state is A″. We could locate a transition state on the S_1 surface for the breaking of the C_{bridge}−C(O) bond at the TD-B3LYP level of theory (**TS1-S1**). This is of C_s symmetry (^{1}A″; *i*256 cm^{-1}), and the breaking bond is stretched to 2.073 Å. The energy of **TS1-S1** is only 3.1 kcal mol^{-1} above the S_1 minimum (**2**-$^1B_1$). Hence, the photochemically accessible first excited state of **2** is very labile and will easily undergo C−C bond cleavage.

As the S_0 and S_1 states are of different symmetry, they will not interact and are allowed to cross within C_s symmetry. In

dx.doi.org/10.1021/jo301622f | J. Org. Chem. 2013, 78, 1851−1857

order to obtain an estimate of the energy and geometry of the S_1/S_0 crossing point, we computed the potential energy surfaces of the S_0 and S_1 states with increasing $C_{bridge}-C(O)$ distance as parameter (Figure 5). Here, the geometries in the S_1 state were optimized (TD-B3LYP/6-311+G**) under the constraint of fixed $C_{bridge}-C(O)$ distances and the energy of the S_0 state at the S_1 geometry is plotted.

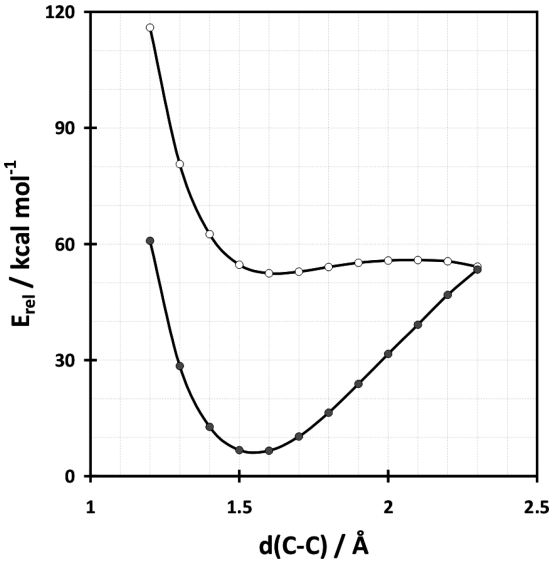

Figure 5. Potential energy curves of the S_0 (filled circles) and S_1 (open circles) states using the $C_{bridge}-C(O)$ distance $d(C-C)$ as reaction coordinate in constraint geometry optimizations of the S_1 state. The final point at 2.3 Å could not be optimized as the energies of the S_1 and S_0 states oscillate; the last point of the optimization before oscillation is used in the plot.

It is seen that the two surfaces come close in energy with increasing $C_{bridge}-C(O)$ distance. The last point at 2.3 Å could not be located properly as the S_1 and S_0 states start to flip and the optimization oscillates. The data point given is the last one before oscillation occurs. The actual conical intersection could not be located as the chosen computational method is unsuitable for such a task. However, at this final point the two states differ by only 1.7 kcal mol^{-1} at the TD-B3LYP/6-311+G** and by only 1.1 kcal mol^{-1} at the CASSCF(2,2)/cc-pVDZ level of theory. Hence, it is clear that the two surfaces cross after passing the transition state on the S_1 surface. Thus, the conical intersection that exists in this part of the surface allows for a transition to the ground state. As the conical intersection is higher in energy than **INT1-S** [13 kcal mol^{-1} at B3LYP, 23 kcal mol^{-1} at CASSCF(2,2)], relaxation of the system to this intermediate on the S_0 surface is conceivable. Hence, the computations on the S_1 surface revealed a mechanism for the fast decomposition of the excited state that involves a low barrier for breaking of the $C_{bridge}-C(O)$ bond and a conical intersection with the S_0 surface that may transport the system into the region of **INT1-S**. As the latter has a low barrier for decarbonylation, the experimental observations of a fast reaction that is complete within 7 ns can be explained.

CONCLUSIONS

The computational study of the Strating–Zwanenburg reaction reveals a number of interesting features of this important transformation in modern acene research. (1) The lowest excited states in the singlet and triplet manifold ($^1B_1$ and $^3B_1$) have stretched carbonyl–bridgehead bonds, $C_{bridge}-C(O)$, and shortened bonds between the carbonyl atoms, (O)C–C(O). This makes reactions that break the former bonds more favorable kinetically and thermodynamically than (O)C–C(O) bond breaking reactions. (2) The bisdecarbonylation of triplet diketone is stepwise; formation of triplet ethylenedione is significantly less favorable than consecutive loss of CO molecules. (3) The bisdecarbonylation on the ground state singlet surface is also stepwise and involves a biradical with a broken $C_{bridge}-C(O)$ bond (**INT1-S**) as the energetically most favorable intermediate. (4) On the S_1 potential energy surface there exists a low-lying transition state (3 kcal mol^{-1} with respect to the S_1 minimum) of C_s symmetry for breaking of the $C_{bridge}-C(O)$ bond. After passing this transition state there is a conical intersection (CI) between the S_0 and S_1 potential energy surface. In the vicinity of the CI the decomposing molecules can cross to and follow the lower energy S_0 surface to a biradical intermediate **INT1-S**. (5) From **INT1-S**, the two CO molecules can be lost simultaneously in a reaction that requires only low (if at all) activation. Alternatively, a transition to the triplet potential energy surface may occur as the diradical is slightly more stable in its triplet electronic state (**INT1-T**). This high-spin system can, however, also lose the two CO molecules in a stepwise reaction that also involves low-barrier bond-breaking processes.

ASSOCIATED CONTENT

Supporting Information

Cartesian coordinates of structures discussed in the text. This material is available free of charge via the Internet at http://pubs.acs.org.

AUTHOR INFORMATION

Corresponding Author

*E-mail: holger.bettinger@uni-tuebingen.de.

Notes

The authors declare no competing financial interest.

ACKNOWLEDGMENTS

The work of the Bettinger research group was supported by the Fonds der Chemischen Industrie and the Deutsche Forschungsgemeinschaft. We are grateful for computer resources provided by bwGRiD. We thank Rafael Bula for performing preliminary calculations. Contribution no. 881 from the Center for Photochemical Sciences.

REFERENCES

(1) Wang, C.; Dong, H.; Hu, W.; Liu, Y.; Zhu, D. *Chem. Rev.* **2012**, *112*, 2208.
(2) Würthner, F. *Angew. Chem., Int. Ed.* **2001**, *40*, 1037.
(3) Würthner, F.; Schmidt, R. *ChemPhysChem* **2006**, *7*, 793.
(4) Bendikov, M.; Wudl, F.; Perepichka, D. F. *Chem. Rev.* **2004**, *104*, 4891.
(5) Anthony, J. E. *Chem. Rev.* **2006**, *106*, 5028.
(6) Anthony, J. E. *Angew. Chem., Int. Ed.* **2008**, *47*, 452.
(7) Payne, M. M.; Parkin, S. R.; Anthony, J. E. *J. Am. Chem. Soc.* **2005**, *127*, 8028.
(8) Chun, D.; Cheng, Y.; Wudl, F. *Angew. Chem., Int. Ed.* **2008**, *47*, 8380.
(9) Kaur, I.; Stein, N. N.; Kopreski, R. P.; Miller, G. P. *J. Am. Chem. Soc.* **2009**, *131*, 3424.
(10) Qu, H.; Chi, C. *Org. Lett.* **2010**, *12*, 3360.

(11) Kaur, I.; Jazdzyk, M.; Stein, N. N.; Prusevich, P.; Miller, G. P. *J. Am. Chem. Soc.* **2010**, *132*, 1261.
(12) Purushothaman, B.; Bruzek, M.; Parkin, S. R.; Miller, A.-F.; Anthony, J. E. *Angew. Chem., Int. Ed.* **2011**, *50*, 7013.
(13) Uno, H.; Yamashita, Y.; Kikuchi, M.; Watanabe, H.; Yamada, H.; Okujima, T.; Ogawa, T.; Ono, N. *Tetrahedron Lett.* **2005**, *46*, 1981.
(14) Yamada, H.; Yamashita, Y.; Kikuchi, M.; Watanabe, H.; Okujima, T.; Uno, H.; Ogawa, T.; Ohara, K.; Ono, N. *Chem.—Eur. J.* **2005**, *11*, 6212.
(15) Yamada, H.; Kawamura, E.; Sakamoto, S.; Yamashita, Y.; Okujima, T.; Uno, H.; Ono, N. *Tetrahedron Lett.* **2006**, *47*, 7501.
(16) Zhao, Y.; Mondal, R.; Neckers, D. C. *J. Org. Chem.* **2008**, *73*, 5506.
(17) Masumoto, A.; Yamashita, Y.; Go, S.; Kikuchi, T.; Yamada, H.; Okujima, T.; Ono, N.; Uno, H. *Jpn. J. Appl. Phys.* **2009**, *48*, 051505.
(18) Zhao, Y.; Cai, X.; Danilov, E.; Li, G.; Neckers, D. C. *Photochem. Photobiol. Sci.* **2009**, *8*, 34.
(19) Katsuta, S.; Yamada, H.; Okujima, T.; Uno, H. *Tetrahedron Lett.* **2010**, *51*, 1397.
(20) Yamada, H.; Kuzuhara, D.; Ohkubo, K.; Takahashi, T.; Okujima, T.; Uno, H.; Ono, N.; Fukuzumi, S. *J. Mater. Chem.* **2010**, *20*, 3011.
(21) Tönshoff, C.; Bettinger, H. F. *Chem.—Eur. J.* **2012**, *18*, 1789.
(22) Aotake, T.; Ikeda, S.; Kuzuhara, D.; Mori, S.; Okujima, T.; Uno, H.; Yamada, H. *Eur. J. Org. Chem.* **2012**, *2012*, 1723.
(23) Mondal, R.; Adhikari, R. M.; Shah, B. K.; Neckers, D. C. *Org. Lett.* **2007**, *9*, 2505.
(24) Watanabe, M.; Chang, Y. J.; Liu, S.-W.; Chao, T.-H.; Goto, K.; IslamMd, M.; Yuan, C.-H.; Tao, Y.-T.; Shinmyozu, T.; Chow, T. J. *Nat. Chem.* **2012**, *4*, 574.
(25) Mondal, R.; Shah, B. K.; Neckers, D. C. *J. Am. Chem. Soc.* **2006**, *128*, 9612.
(26) Bettinger, H. F.; Mondal, R.; Neckers, D. C. *Chem. Commun.* **2007**, 5209.
(27) Mondal, R.; Tönshoff, C.; Khon, D.; Neckers, D. C.; Bettinger, H. F. *J. Am. Chem. Soc.* **2009**, *131*, 14281.
(28) Tönshoff, C.; Bettinger, H. F. *Angew. Chem., Int. Ed.* **2010**, *49*, 4125.
(29) Strating, J.; Zwanenburg, B.; Wagenaar, A.; Udding, A. C. *Tetrahedron Lett.* **1969**, 125.
(30) Gream, G. E.; Price, J. C.; Ramsay, C. C. R. *Aust. J. Chem.* **1969**, *22*, 1229.
(31) Turro, N. J.; Lee, T.-J. *J. Am. Chem. Soc.* **1969**, *91*, 5651.
(32) Rubin, M. B.; Gutman, A. L. *J. Org. Chem.* **1986**, *51*, 2511.
(33) Park, J. W.; Kim, E. K.; Park, K. K. *Bull. Korean Chem. Soc.* **2002**, *23*, 1229.
(34) Hassoon, S.; Rubin, M. B.; Speiser, S. *J. Photochem.* **1984**, *26*, 295.
(35) Rubin, M. B. *J. Am. Chem. Soc.* **1981**, *103*, 7791.
(36) Rubin, M. B.; Kapon, M. *J. Photochem. Photobiol. A: Chem.* **1999**, *124*, 41.
(37) Rubin, M. B.; Patyk, A.; Sander, W. *Tetrahedron Lett.* **1988**, *29*, 6641.
(38) Schröder, D.; Heinemann, C.; Schwarz, H.; Harvey, J. N.; Dua, S.; Blanksby, S. J.; Bowie, J. H. *Chem.—Eur. J.* **1998**, *4*, 2550.
(39) Talbi, D.; Chandler, G. S. *J. Phys. Chem. A* **2000**, *104*, 5872.
(40) Mondal, R.; Okhrimenko, A. N.; Shah, B. K.; Neckers, D. C. *J. Phys. Chem. B* **2008**, *112*, 11.
(41) Becke, A. D. *J. Chem. Phys.* **1993**, *98*, 5648.
(42) Lee, C.; Yang, W.; Parr, R. G. *Phys. Rev. B* **1988**, *37*, 785.
(43) Stephens, P. J.; Devlin, F. J.; Chabalowski, C. F.; Frisch, M. J. *J. Phys. Chem.* **1994**, *98*, 11623.
(44) Frisch, M. J.; Trucks, G. W.; Schlegel, H. B.; Scuseria, G. E.; Robb, M. A.; Cheeseman, J. R.; Scalmani, G.; Barone, V.; Mennucci, B.; Petersson, G. A.; Nakatsuji, H.; Caricato, M.; Li, X.; Hratchian, H. P.; Izmaylov, A. F.; Bloino, J.; Zheng, G.; Sonnenberg, J. L.; Hada, M.; Ehara, M.; Toyota, K.; Fukuda, R.; Hasegawa, J.; Ishida, M.; Nakajima, T.; Honda, Y.; Kitao, O.; Nakai, H.; Vreven, T.; Montgomery, J. A., Jr.; Peralta, J. E.; Ogliaro, F.; Bearpark, M.; Heyd, J. J.; Brothers, E.; Kudin, K. N.; Staroverov, V. N.; Kobayashi, R.; Normand, J.; Raghavachari, K.; Rendell, A.; Burant, J. C.; Iyengar, S. S.; Tomasi, J.; Cossi, M.; Rega, N.; Millam, J. M.; Klene, M.; Knox, J. E.; Cross, J. B.; Bakken, V.; Adamo, C.; Jaramillo, J.; Gomperts, R.; Stratmann, R. E.; Yazyev, O.; Austin, A. J.; Cammi, R.; Pomelli, C.; Ochterski, J. W.; Martin, R. L.; Morokuma, K.; Zakrzewski, V. G.; Voth, G. A.; Salvador, P.; Dannenberg, J. J.; Dapprich, S.; Daniels, A. D.; Farkas, Ö.; Foresman, J. B.; Ortiz, J. V.; Cioslowski, J.; Fox, D. J. *Gaussian 09*, Revision A.02, Wallingford, CT, 2009.
(45) Hehre, W. J.; Ditchfield, R.; Pople, J. A. *J. Chem. Phys.* **1972**, *56*, 2257.
(46) Hariharan, P. C.; Pople, J. A. *Theor. Chim. Acta* **1973**, *28*, 213.
(47) Krishnan, R.; Binkley, J. S.; Seeger, R.; Pople, J. A. *J. Chem. Phys.* **1980**, *72*, 650.
(48) Bauernschmitt, R.; Ahlrichs, R. *Chem. Phys. Lett.* **1996**, *256*, 454.
(49) Stratmann, R. E.; Scuseria, G. E.; Frisch, M. J. *J. Chem. Phys.* **1998**, *109*, 8218.
(50) Furche, F.; Ahlrichs, R. *J. Chem. Phys.* **2002**, *117*, 7433.
(51) Bauernschmitt, R.; Ahlrichs, R. *J. Chem. Phys.* **1996**, *104*, 9047.
(52) Raghavachari, K.; Trucks, G. W.; Pople, J. A.; Head-Gordon, M. *Chem. Phys. Lett.* **1989**, *157*, 479.
(53) Dunning, T. H. *J. Chem. Phys.* **1989**, *90*, 1007.
(54) Nakano, H. *J. Chem. Phys.* **1993**, *99*, 7983.
(55) Nakano, H. *Chem. Phys. Lett.* **1993**, *207*, 372.
(56) Nakano, H.; Hirao, K.; Gordon, M. S. *J. Chem. Phys.* **1998**, *108*, 5660.
(57) Hirao, K. *Chem. Phys. Lett.* **1992**, *190*, 374.
(58) Hirao, K. *Chem. Phys. Lett.* **1992**, *196*, 397.
(59) Hirao, K. *Int. J. Quantum Chem.* **1992**, *S26*, 517.
(60) Hirao, K. *Chem. Phys. Lett.* **1993**, *201*, 59.
(61) Pulay, P.; Hamilton, T. P. *J. Chem. Phys.* **1988**, *88*, 4926.
(62) Schmidt, M. W.; Baldridge, K. K.; Boatz, J. A.; Elbert, S. T.; Gordon, M. S.; Jensen, J. H.; Koseki, S.; Matsunaga, N.; Nguyen, K. A.; Su, S.; Windus, T. L.; Dupuis, M.; Montgomery, J. A. *J. Comput. Chem.* **1993**, *14*, 1347.
(63) Padhye, M. R.; McGlynn, S. P.; Kasha, M. *J. Chem. Phys.* **1956**, *24*, 588.
(64) Korkin, A. A.; Balkova, A.; Bartlett, R. J.; Boyd, R. J.; Schleyer, P. v. R. *J. Phys. Chem.* **1996**, *100*, 5702.